Electronic Supplementary Material (ESI) for Physical Chemistry Chemical Physics.

Supplementary Information for:

Distinct Doorway States Lead to Triplet Excited State Generation in Epigenetic RNA Nucleosides

Danhong Wang[a], Xueli Wang[a]*, Peipei Jin[a], Yusong Zhou[a], Menghui Jia[a], Haifeng Pan[a], Zhenrong Sun[a] and Jinquan Chen[a] [b]*

[a] D. Wang, X. Wang, P. Jin, Y. Zhou, M. Jia, Prof. H. Pan, Prof. Z. Sun, Prof. J. Chen

State Key Laboratory of Precision Spectroscopy

East China Normal University

Shanghai 200241, China

E-mail: xlwang@lps.ecnu.edu.cn; jqchen@lps.ecnu.edu.cn

[b] Prof. J. Chen

Collaborative Innovation Center of Extreme Optics

Shanxi University

Taiyuan, Shanxi 030006, China

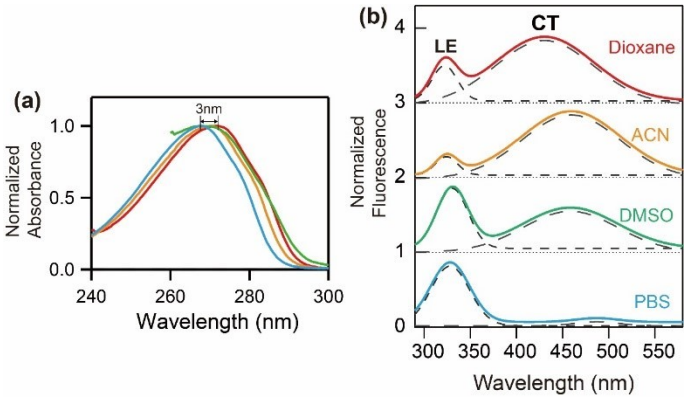

Figure S1. (a) Normalized steady-state absorption spectra and (b) normalized fluorescence emission spectra of hm6A under 275 nm excitation. Solvent signals have been corrected in all spectra. Emission of the CT state is determined by solvent polarity dependent experiments.

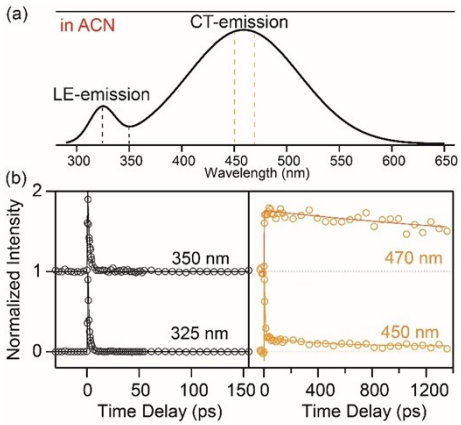

Figure S2. (a) Steady-state emission spectra of hm6A in ACN. The wavelength marked by dotted straight lines are detected in fluorescence up-conversion measurement. (b) Normalized fluorescence kinetics at indicated wavelength. Long-lived CT emission are seen at the lower energy emission band centered at 465 nm.

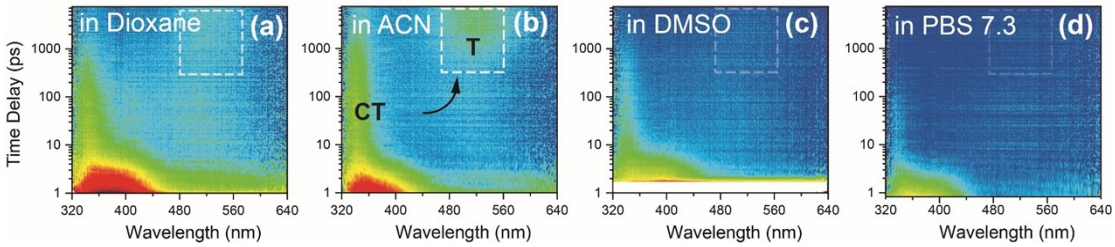

Figure S3. 2D color filled contour of fs-TA spectra for hm6A in four different solvents. Polarity sequence from small to large: Dioxane < ACN < DMSO< PBS. The fitting lifetime constants are listed in Table S1.

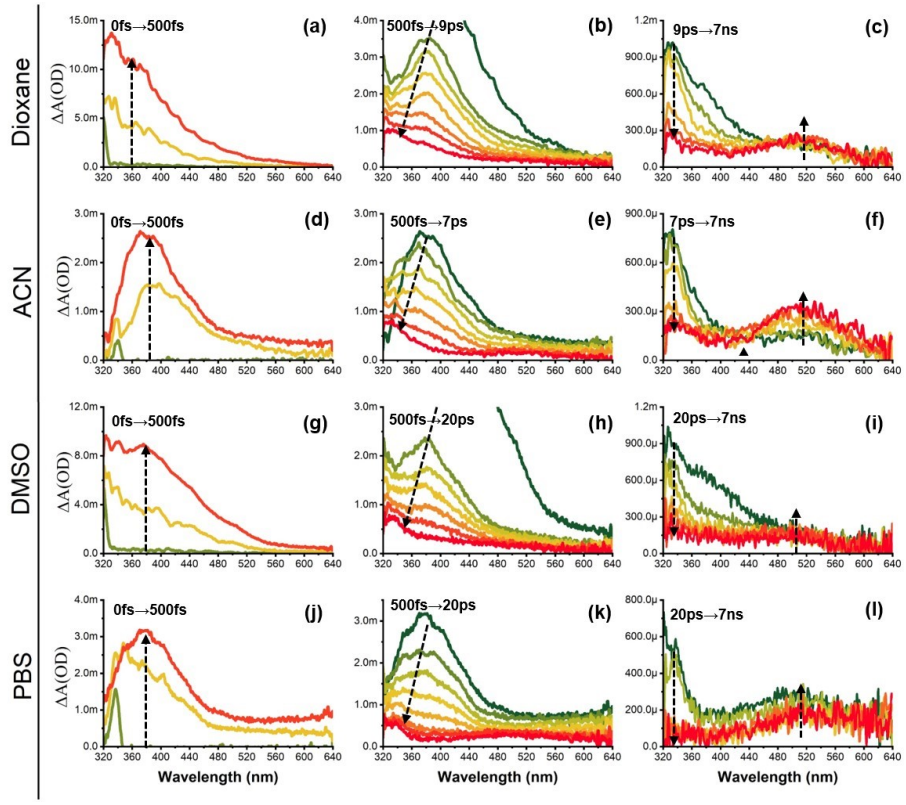

Figure S4. TA spectra of hm6A in Dioxane (a-c), ACN (d-f), DMSO (g-i) and PBS (j-l) under 275 nm excitation. TA signals of hm6A in the first 500 fs is strongly mixed with nonlinear solvent response signals. Thus, TA Spectra after 500 fs are meaningful for hm6A.

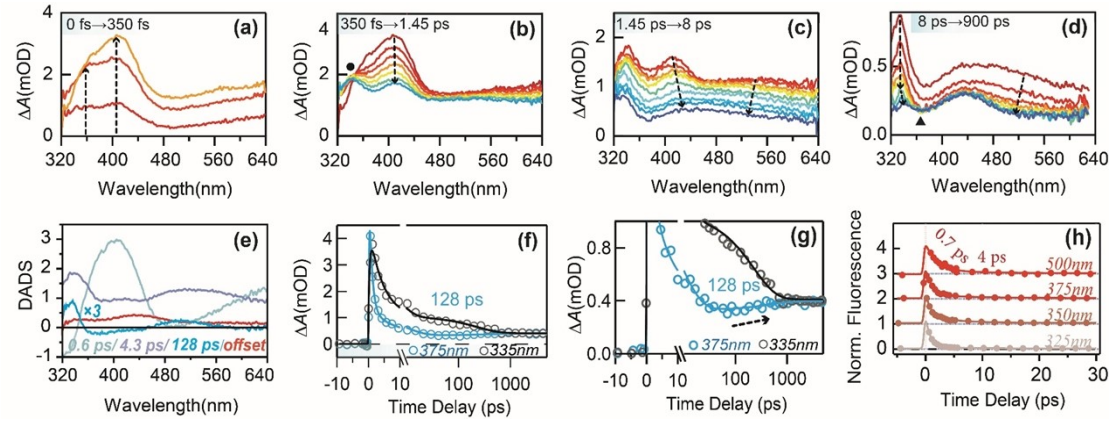

Figure S5. TA spectra (a-g) and fluorescence up-conversion measurement (h) of f6A in PBS under 267 nm excitation. (a-d) TA spectra with indicated time delays. Dotted arrows point out the evolution direction. (e) Decay associated difference spectra (DADS) with three lifetime constants and one offset. Corresponding lifetime constants are marked in DADS panel. For easy viewing, the 128 ps DADS line is magnified by a factor of three. (f) (g) Kinetic decay curves at 335 nm (black) and 378 nm (blue). (h) Normalized fluorescence kinetics at indicated probe wavelength measured by up-conversion technique.

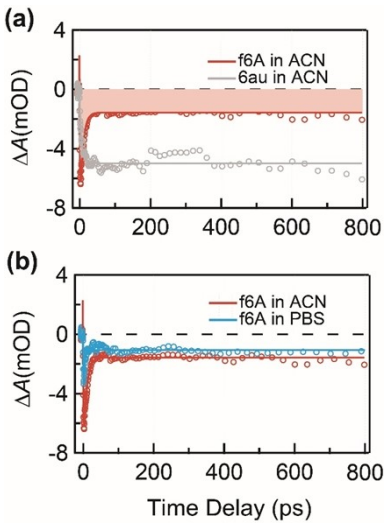

Figure S6. (a) Triplet state quantum yield for f6A in ACN is determined to be 27% under 267 nm excitation. 6-azaU with 100% triplet state yield is used as reference [1]. This method has been reported before [2]. (b) Compared experiment results suggest similar triplet yield of f6A in PBS.

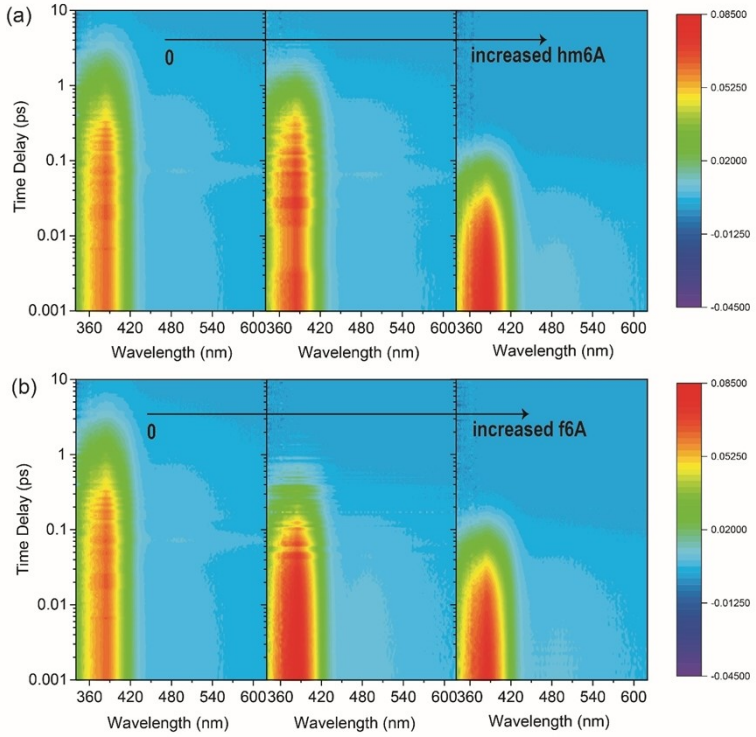

Figure S7. 2D color filled contour of ns-TA spectra for ApOMe with increasing amounts of hm6A and f6A in ACN solvent under N2 atmosphere.

Table S1. Fitted lifetimes of hm6A and f6A in ACN abstracted from TA and UPC measurements. The lifetime constants of offset components in N_2/Air-saturated are given.

Method	mol.	τ_1 (ps)	τ_2 (ps)	τ_3 (ns)	τ_4 (ns; N2/ Air) [a]
TA （320-640 nm）	hm6A(ACN)	0.4±0.2	2.1±0.2	1.21±0.02	180±10/26±5
	hm6A(Dioxane)	0.2±0.1	2.6±0.1	1.29±0.12	offset
	hm6A(DMSO)	0.3±0.1	3.7±0.2	0.95±0.15	offset
	hm6A(PBS)	0.7±0.1	2.6±0.4	0.024±0.019	offset
	f6A(ACN)	0.4±0.3	7.3±0.3	0.13±0.02	348±18/95±10
	f6A(PBS)	0.6±0.2	4.3±0.3	0.13±0.05	offset
TA （255 nm）	f6A(ACN)	0.4±0.1	8.1±0.2	-	long-lived
	f6A(PBS)	0.6±0.2	4.5±0.2	-	long-lived
UPC	hm6A(ACN)	0.6±0.2	2.3±0.2	long-lived	-
	f6A(ACN)	0.4±0.2	7.6±0.1	-	-
	f6A(PBS)	0.7±0.2	4.0±0.1	-	-

[a] The lifetime constant τ_4 of two molecules in ACN solvent were obtained from ns-TA.

Table S2. Main information of optimized ground and first excited electronic state geometries of hm6A and f6A.

S_{0min} of hm6A		
Level of theory	**ωB97XD/6-311++g (d, p)/PCM**	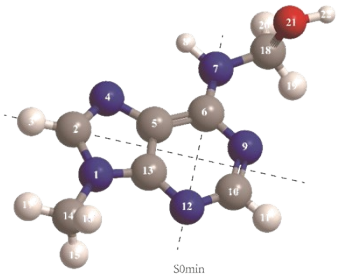
Relative energy (eV)	0.00	
C_6-N_7 distance (Å)	1.357	
N_7-C_{18} distance (Å)	1.427	
C_{18}-O_{21} distance (Å)	1.423	
C_5-C_6-N_7 angle (°)	121.1	
C_6-N_7-C_{18} angle (°)	123.8	
N_7-C_{18}-O_{21} angle (°)	109.3	
N_1-C_{13}-C_5-C_6 dihedral (°)	179.9	
C_{13}-C_5-C_6-N_7 dihedral (°)	178.6	
C_5-C_6-N_7-C_{18} dihedral (°)	171.5	
C_6-N_7-C_{18}-O_{21} dihedral (°)	-82.51	
Level of theory	**B3LYP-D3BJ/6-311++g (d, p)/PCM**	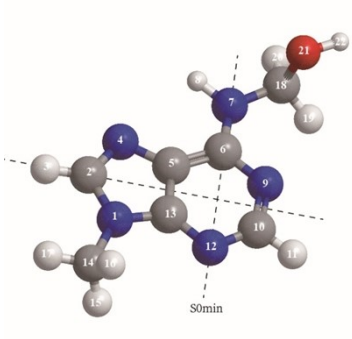
Relative energy (eV)	0.00	
C_6-N_7 distance (Å)	1.361	
N_7-C_{18} distance (Å)	1.429	
C_{18}-O_{21} distance (Å)	1.437	
C_5-C_6-N_7 angle (°)	121.2	
C_6-N_7-C_{18} angle (°)	123.9	
N_7-C_{18}-O_{21} angle (°)	109.3	
N_1-C_{13}-C_5-C_6 dihedral (°)	179.8	
C_{13}-C_5-C_6-N_7 dihedral (°)	178.5	
C_5-C_6-N_7-C_{18} dihedral (°)	171.5	
C_6-N_7-C_{18}-O_{21} dihedral (°)	-83.09	

S_1LE_{min} of hm6A		
Level of theory	**ωB97XD/6-311++g (d, p)/PCM**	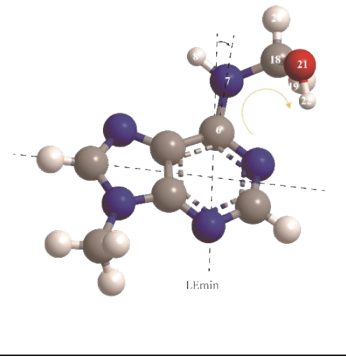
Relative energy (eV)	3.7 (3.9 eV in exp.)	
C_6-N_7 distance (Å)	1.380	
N_7-C_{18} distance (Å)	1.439	
C_{18}-O_{21} distance (Å)	1.415	
C_5-C_6-N_7 angle (°)	117.2	
C_6-N_7-C_{18} angle (°)	122.3	
N_7-C_{18}-O_{21} angle (°)	113.8	
N_1-C_{13}-C_5-C_6 dihedral (°)	-174.85	
C_{13}-C_5-C_6-N_7 dihedral (°)	**-145.5**	
C_5-C_6-N_7-C_{18} dihedral (°)	**147.9**	
C_6-N_7-C_{18}-O_{21} dihedral (°)	-69.03	
Level of theory	**B3LYP-D3BJ/6-311++g (d, p)/PCM**	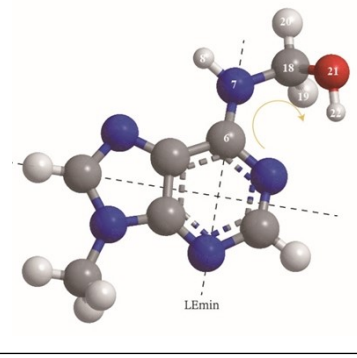
Relative energy (eV)	3.9 (3.9 eV in exp.)	
C_6-N_7 distance (Å)	1.357	
N_7-C_{18} distance (Å)	1.451	
C_{18}-O_{21} distance (Å)	1.416	
C_5-C_6-N_7 angle (°)	120.5	
C_6-N_7-C_{18} angle (°)	121.7	
N_7-C_{18}-O_{21} angle (°)	112.5	
N_1-C_{13}-C_5-C_6 dihedral (°)	-172.5	
C_{13}-C_5-C_6-N_7 dihedral (°)	**178.4**	
C_5-C_6-N_7-C_{18} dihedral (°)	**179.4**	
C_6-N_7-C_{18}-O_{21} dihedral (°)	-62.58	

S_1CT_{min} of hm6A		
Level of theory	**ωB97XD/6-311++g (d, p)/PCM**	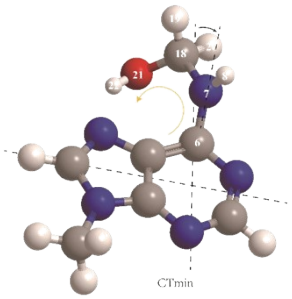
Relative energy (eV)	2.97 (2.69 eV in exp.)	
C_6-N_7 distance (Å)	1.396	
N_7-C_{18} distance (Å)	1.457	
C_{18}-O_{21} distance (Å)	1.386	
C_5-C_6-N_7 angle (°)	111.4	
C_6-N_7-C_{18} angle (°)	124.2	
N_7-C_{18}-O_{21} angle (°)	113.3	
N_1-C_{13}-C_5-C_6 dihedral (°)	-177.0	
C_{13}-C_5-C_6-N_7 dihedral (°)	**-139.5**	
C_5-C_6-N_7-C_{18} dihedral (°)	**-78.62**	
C_6-N_7-C_{18}-O_{21} dihedral (°)	**19.34**	
Level of theory	**B3LYP-D3BJ/6-311++g (d, p)/PCM**	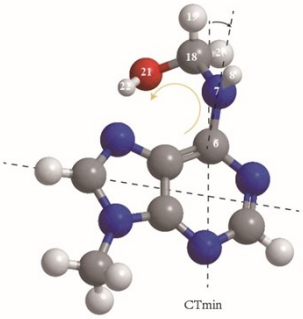
Relative energy (eV)	3.00 (2.69 eV in exp.)	
C_6-N_7 distance (Å)	1.421	
N_7-C_{18} distance (Å)	1.451	
C_{18}-O_{21} distance (Å)	1.394	
C_5-C_6-N_7 angle (°)	113.9	
C_6-N_7-C_{18} angle (°)	122.7	
N_7-C_{18}-O_{21} angle (°)	112.0	
N_1-C_{13}-C_5-C_6 dihedral (°)	-174.3	
C_{13}-C_5-C_6-N_7 dihedral (°)	**-154.1**	
C_5-C_6-N_7-C_{18} dihedral (°)	**-83.62**	
C_6-N_7-C_{18}-O_{21} dihedral (°)	**31.21**	

S_{0min} of f6A		
Level of theory	**ωB97XD/6-311++g (d, p)/PCM**	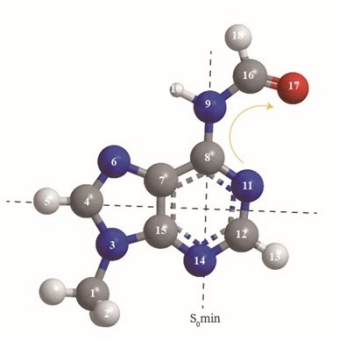
Relative energy (eV)	0.00	
C_8-N_9 distance (Å)	1.386	
N_9-C_{16} distance (Å)	1.374	
C_{16}-O_{17} distance (Å)	1.207	
C_7-C_8-N_9 angle (°)	118.4	
C_8-N_9-C_{16} angle (°)	130.4	
N_9-C_{16}-O_{17} angle (°)	127.1	
N_3-C_{15}-C_7-C_8 dihedral (°)	179.9	
C_{15}-C_7-C_8-N_9 dihedral (°)	-180.0	
C_7-C_8-N_9-C_{16} dihedral (°)	177.4	
C_8-N_9-C_{16}-O_{17} dihedral (°)	0.058	
Level of theory	**B3LYP-D3BJ/6-311++g (d, p)/PCM**	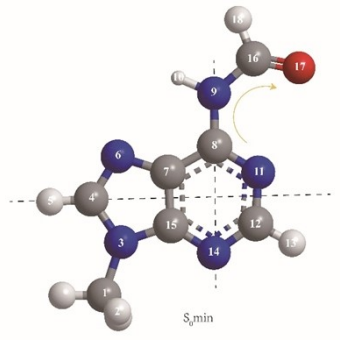
Relative energy (eV)	0.00	
C_8-N_9 distance (Å)	1.389	
N_9-C_{16} distance (Å)	1.376	
C_{16}-O_{17} distance (Å)	1.212	
C_7-C_8-N_9 angle (°)	118.4	
C_8-N_9-C_{16} angle (°)	130.7	
N_9-C_{16}-O_{17} angle (°)	127.2	
N_3-C_{15}-C_7-C_8 dihedral (°)	-179.9	
C_{15}-C_7-C_8-N_9 dihedral (°)	178.0	
C_7-C_8-N_9-C_{16} dihedral (°)	-178.5	
C_8-N_9-C_{16}-O_{17} dihedral (°)	-0.055	

S_{1min} of f6A		
Level of theory	**ωB97XD/6-311++g (d, p)/PCM**	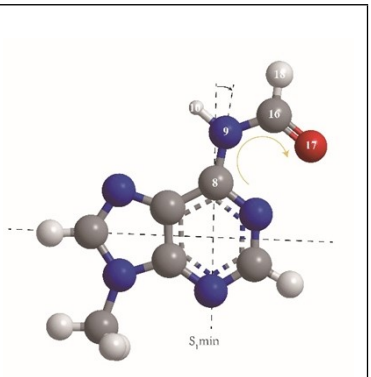
Relative energy (eV)	3.13	
C_8-N_9 distance (Å)	1.353	
N_9-C_{16} distance (Å)	1.355	
C_{16}-O_{17} distance (Å)	1.266	
C_7-C_8-N_9 angle (°)	128.2	
C_8-N_9-C_{16} angle (°)	120.3	
N_9-C_{16}-O_{17} angle (°)	120.6	
N_3-C_{15}-C_7-C_8 dihedral (°)	-180.0	
C_{15}-C_7-C_8-N_9 dihedral (°)	180.0	
C_7-C_8-N_9-C_{16} dihedral (°)	180.0	
C_8-N_9-C_{16}-O_{17} dihedral (°)	-0.009	
Level of theory	**B3LYP-D3BJ/6-311++g (d, p)/PCM**	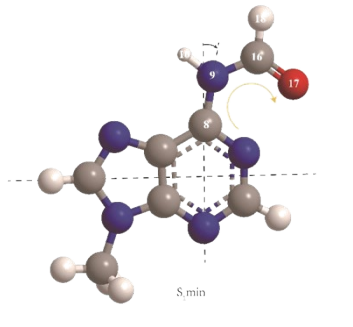
Relative energy (eV)	2.83	
C_8-N_9 distance (Å)	1.366	
N_9-C_{16} distance (Å)	1.350	
C_{16}-O_{17} distance (Å)	1.268	
C_7-C_8-N_9 angle (°)	127.7	
C_8-N_9-C_{16} angle (°)	120.6	
N_9-C_{16}-O_{17} angle (°)	121.0	
N_3-C_{15}-C_7-C_8 dihedral (°)	180.0	
C_{15}-C_7-C_8-N_9 dihedral (°)	180.0	
C_7-C_8-N_9-C_{16} dihedral (°)	-180.0	
C_8-N_9-C_{16}-O_{17} dihedral (°)	-0.028	

Table S3. Vertical excitation energies and transitions of hm6A in FC region, calculated with different functionals at TD-DFT/PCM /6-311++g (d, p) level of the theory.

State	**ωB97XD**		State	**B3LYP-D3BJ**	
	Transition [a] (Contribution)	Energy (eV)/oscillator strength		Transition (Contribution)	Energy (eV)/oscillator strength
$T_1(\pi\pi^*)$	H -> L	3.63/ 0	$T_1(\pi\pi^*)$	H -> L	3.47/0
$T_2(\pi\pi^*)$	H -> L+4	4.57/ 0	$T_2(\pi\pi^*)$	H -> L+1	4.35/0
$T_3(\pi\pi^*\&n\pi^*)$	H-1 -> L (-0.325) H-2 -> L (0.392)	5.06/ 0	$T_3(n\pi^*)$	H-1 -> L	4.71/0
$T_4(\pi\pi^*\&n\pi^*)$	H-1 -> L (0.514) H-2 -> L (0.341)	5.11/ 0	$T_4(\pi\pi^*)$	H-2 -> L	4.81/0
$S_1(\pi\pi^*)$	H -> L	5.20 (4.51 in exp.)/ 0.428	$S_1(\pi\pi^*)$	H -> L	4.82(4.51 in exp.)/0.345
$T_5(n\pi^*)$	H-2 -> L	5.30/ 0	$S_2(n\pi^*)$	H-1 -> L	5.00/0.020
$S_2(n\pi^*)$	H-1 -> L	5.41/ 0.013	$T_5(\pi\pi^*)$	H-2 -> L (0.367) H -> L+5 (0.301)	5.01/0
$S_3(\pi\pi^*)$	H -> L+4	5.44/ 0.017	$S_3(\pi\pi^*)$	H -> L+1	5.11/0.042
$T_6(n\pi^*)$	H-2 -> L+4	5.46/ 0	$T_6(n\pi^*\&\pi\pi^*)$	H-1 -> L+1 (0.460) H-2 -> L+1 (-0.403)	5.17/0
$T_7(\pi\pi^*)$	H-1 -> L+4	5.20/ 0	$T_7(n\pi^*\&\pi\pi^*)$	H-1 -> L+1 (0.462) H-2 -> L+1 (0.430)	5.20/0

[a] H refers to HOMO and L refers to LUMO.

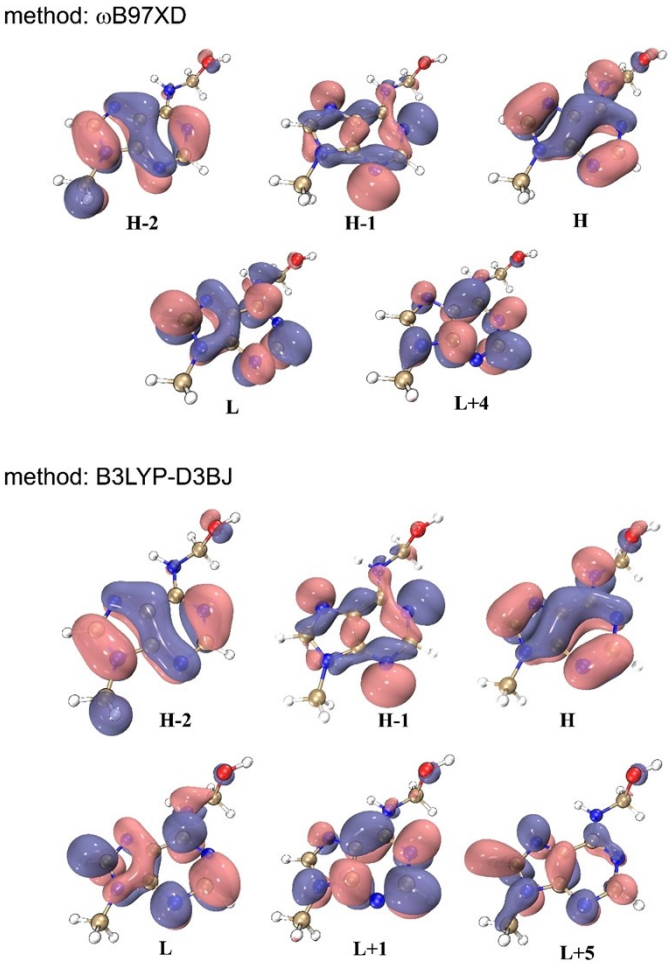

Figure S8. Corresponding HOMO-LUMO orbitals (iso=0.03) that contribute to the vertical transitions of hm6A in ACN at FC region.

Table S4. Vertical excitation energies and transitions of f6A in ACN at FC region, calculated with different functionals at TD-DFT/PCM /6-311++g (d, p) level of the theory.

State	ωB97XD		State	B3LYP-D3BJ	
	Transition [a] (Contribution)	Energy (eV)/oscillator strength		Transition (Contribution)	Energy (eV)/oscillator strength
$T_1(\pi\pi^*)$	H -> L	3.53/0	$T_1(\pi\pi^*)$	H -> L	3.35/ 0
$T_2(n\pi^*)$	H-1 -> L	4.34/0	$T_2(n\pi^*)$	H-1 -> L	3.95/ 0
$T_3(\pi\pi^*)$	H -> L+2	4.64/0	$S_1(n\pi^*)$	H-1 -> L	4.26/ 0.0001
$S_1(n\pi^*)$	H-1 -> L	4.70/0.0001	$T_3(\pi\pi^*)$	H -> L+1 (0.567) H-2 -> L (0.314)	4.43/ 0
$T_4(\pi\pi^*)$	H-2 -> L	4.84/0	$T_4(\pi\pi^*)$	H-2 -> L (0.560) H -> L+1 (-0.332)	4.52/ 0
$T_5(n\pi^*)$	H-3 -> L	4.93/0	$T_5(n\pi^*)$	H-3 -> L	4.58/ 0
$S_2(\pi\pi^*)$	H -> L	5.01 (4.51 in exp.)/ 0.504	$S_2(\pi\pi^*)$	H -> L	4.63 (4.51 in exp.)/ 0.4397
$T_6(\pi\pi^*)$	H-4 -> L (0.338) H-2 -> L (0.330)	5.15/0	$T_6(\pi\pi^*)$	H -> L+3 (0.424) H-4 -> L (0.421)	4.84/ 0
$T_7(n\pi^*)$	H-1 -> L+2	5.33/0	$T_7(n\pi^*)$	H-1 -> L+1	4.94/ 0
$S_3(n\pi^*)$	H-3 -> L	5.37/0.002	$S_3(n\pi^*)$	H-3 -> L	4.99/ 0.001

[a] H refers to HOMO and L refers to LUMO.

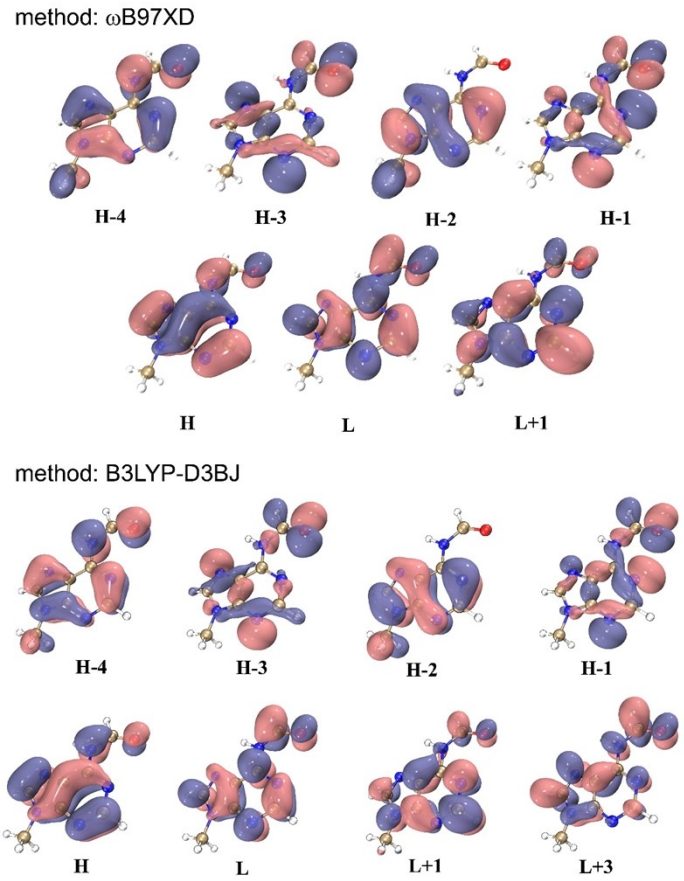

Figure S9. Corresponding HOMO-LUMO orbitals (iso=0.03) that contribute to the vertical transitions of f6A in ACN at FC region.

Table S5. Relative energies and spin-orbit couplings between the lowest CT singlet and triplet states of hm6A calculated at optimized CT geometry with different functionals by the 6-311++g (d, p)/PCM theory, conducted in ORCA software.

State	Transition (Contribution) [a]	Energy (eV)	ΔE (eV)	SOC (cm^{-1})	Functional
$CT_{min}(\pi\pi^*)$	H -> L (0.909)	3.03	-	-	**ωB97X-D3**
$T_1(\pi\pi^*)$	H -> L	2.02	1.01	1.36	
$T_2(\pi\pi^*)$	H-1 -> L	3.58	-0.55	4.13	
$T_3(n\pi^*)$	H-2 -> L	3.93	-0.9	5.43	
$T_4(n\pi^*)$	H-3 -> L	4.07	-1.04	3.51	
$T_5(\pi\pi^*)$	H -> L+4	4.4	-1.37	1.90	
$CT_{min}(\pi\pi^*)$	H -> L (0.956)	2.70	-	-	**B3LYP/G-D3BJ**
$T_1(\pi\pi^*)$	H -> L	2.51	0.19	2.36	
$T_2(\pi\pi^*)$	H-1 -> L	3.10	-0.4	3.25	
$T_3(n\pi^*)$	H-2 -> L	3.72	-1.02	7.66	
$T_4(\pi\pi^*)$	H-3 -> L	3.93	-1.23	3.79	
$T_5(\pi\pi^*)$	H -> L+1	4.22	-1.52	1.38	

[a] H refers to HOMO and L refers to LUMO.

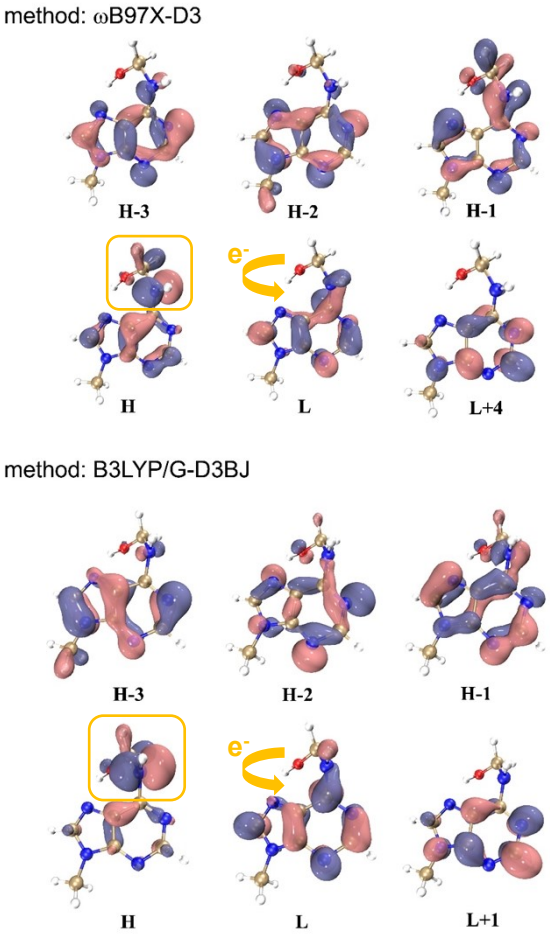

Figure S10. Corresponding HOMO-LUMO orbitals (iso=0.05) that contribute to the vertical transitions of hm6A in ACN at CT_{min} region.

Table S6. Relative energies and spin-orbit couplings between the lowest singlet S_1 and triplet states of f6A calculated at optimized S_1 geometry with different functionals by the 6-311++g (d, p)/PCM theory, conducted in ORCA software.

State	Transition [a]	Energy (eV)	ΔE (eV)	SOC (cm^{-1})	Functional
$S_{1min}(n\pi^*)$	H -> L	3.18	-	-	**ωB97X-D3**
$T_1(n\pi^*)$	H -> L	2.86	0.32	0.26	
$T_2(\pi\pi^*)$	H-1 -> L	3.40	-0.22	9.86	
$T_3(n\pi^*)$	H -> L+4	4.30	-1.12	2.75	
$T_4(\pi\pi^*)$	H-2 -> L	4.54	-1.36	9.77	
$T_5(n\pi^*)$	H -> L+7	4.57	-1.39	2.45	
$S_{1min}(n\pi^*)$	H -> L	2.76	-	-	**B3LYP/G-D3BJ**
$T_1(n\pi^*)$	H -> L	2.49	0.27	0.27	
$T_2(\pi\pi^*)$	H-1 -> L	3.14	-0.38	9.83	
$T_3(n\pi^*)$	H -> L+1	3.75	-1	1.87	
$T_4(\pi\pi^*)$	H-2 -> L	4.16	-1.4	8.22	
$T_5(n\pi^*)$	H -> L+3	4.17	-1.41	4.45	

[a] H refers to HOMO and L refers to LUMO.

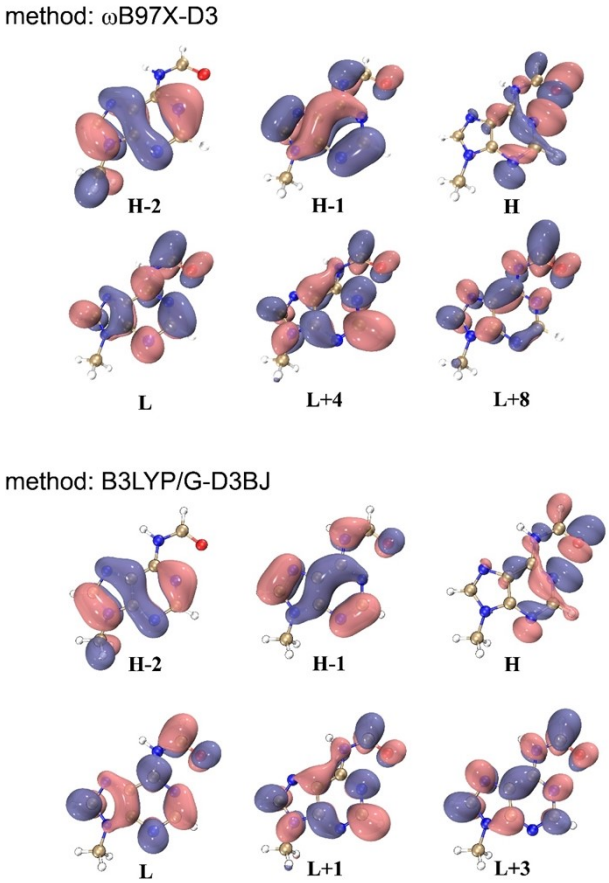

Figure S11. Corresponding HOMO-LUMO orbitals (iso=0.03) that contribute to the vertical transitions of f6A in ACN at S_{1min} region.

Table S7. Key indexes of the optimized structure CT_{min} of hm6A obtained from hole-electron distribution analysis.

	Sr[a]	D(Å)[b]	t(Å)[c]
$CT_{min} \rightarrow S_0$	0.46	1.90	0.45

[a] **Sr**-index can reflect the degree of overlap between electron and hole distribution, with a value of 0 representing no overlap at all and a value of 1 representing complete overlap. [b] **D**-index can characterize the center-of-mass spacing of electrons and holes. The smaller the value, the smaller the overlap of electron holes and the more separated they are. [c] **t**-index can assess the degree of separation of holes and electrons. Generally, a t-index > 0 implies that the separation of holes and electrons is more adequate due to CT, since the holes and electrons are farther apart from the center of mass and their average extension in this direction is not so high. Conversely, a t-index < 0 would suggest that there is no significant separation of holes and electrons in the CT direction. Detailed information of hole-electron analysis can be found in Lu's paper.[3]

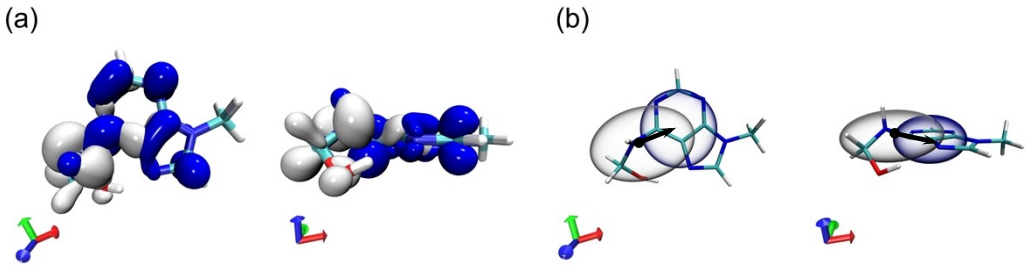

Figure S12. (a) Isosurface of hole and electron distribution including front view and top view. White surface means the hole distribution and blue surface means electron distribution. (iso=0.002) (b) Isosurface of C_{ele} and C_{hole} functions were shown to check the hole-electron distribution more intuitively. White transparent surface means C_{ele} function distribution and blue transparent surface means C_{hole} function distribution. (iso=0.0002) Additionally, the centers of the two equivalence surfaces correspond to the center-of-mass positions of the hole and electron respectively. (Detailed information of definition of functions can also be found in Lu's paper.[3] It is clearly shown that hole and electron distribution is separated in space at this optimized state CT_{min}. Hole-electron analysis and orbital information demonstrate it is a luminescent state with charge transfer characteristics, which is consistent with our experimental conclusion.

Data files of the optimized structure

S_{0min} of 9Mehm6A

ωB97X-D3

0 1

N	2.50521300	-0.33216000	0.10280700
C	2.11120700	-1.64064600	0.03283200
H	2.83596900	-2.44041600	0.09175800
N	0.81977000	-1.80068900	-0.10643600
C	0.33055100	-0.51179600	-0.12913300
C	-0.96756300	0.01470100	-0.25054200
N	-2.04221300	-0.79826100	-0.40961400
H	-1.86993500	-1.78747000	-0.31883500
N	-1.12183300	1.34305300	-0.23205700
C	-0.03366500	2.11546000	-0.10504900
H	-0.22224500	3.18505200	-0.09923600
N	1.23316100	1.74356600	0.01657700
C	1.36074900	0.41103000	-0.00079800
C	3.85543400	0.17885300	0.25722400
H	4.11593900	0.80822000	-0.59388600
H	3.93178800	0.76059100	1.17603600
H	4.54274700	-0.66381900	0.30585900
C	-3.39467300	-0.34526000	-0.36407700
H	-3.45586500	0.62899000	-0.85206100
H	-4.01195000	-1.06831300	-0.90340200
O	-3.81443200	-0.25079200	0.99259800
H	-4.68191300	0.16089300	1.01129900

B3LYP-D3BJ

0 1

N	2.51587300	-0.33489300	0.10369500
C	2.12047800	-1.65099300	0.03118100
H	2.84290900	-2.45151700	0.08903700
N	0.82122500	-1.80398200	-0.10976300
C	0.32882700	-0.51165800	-0.13125200
C	-0.97056900	0.01673600	-0.25254800
N	-2.05055700	-0.79598400	-0.41482700
H	-1.87937500	-1.78677000	-0.32429300
N	-1.12452600	1.35111100	-0.23216800
C	-0.03511600	2.12562900	-0.10345200
H	-0.22121600	3.19501900	-0.09593800
N	1.23836700	1.74879300	0.01914300
C	1.36789600	0.41511300	0.00004500
C	3.87158200	0.17572200	0.25999700
H	4.13338500	0.80684900	-0.58945200
H	3.94863700	0.75680800	1.17921300
H	4.55703800	-0.66806200	0.30756600
C	-3.40456500	-0.34112700	-0.36918900
H	-3.46230500	0.64041800	-0.83986400
H	-4.02434400	-1.05594000	-0.91533500
O	-3.83194300	-0.26241600	1.00013400
H	-4.71305700	0.13067100	1.01673800

S_{1min} of 9Mehm6A

ωB97X-D3

0 1

N	2.45779700	-0.19823200	0.19367300
C	2.24713200	-1.52852000	0.04578900
H	3.03032900	-2.25598800	0.19412900
N	0.97473600	-1.81467700	-0.28424900
C	0.34761400	-0.63759200	-0.30265900
C	-1.00723900	-0.22813900	-0.66986600

N	-2.04363000	-1.05194600	-0.27932700
H	-1.81609800	-2.00970700	-0.05411800
N	-1.26285200	1.11906800	-0.67656800
C	-0.32596500	1.97851500	-0.37643900
H	-0.59188600	3.03002800	-0.40386700
N	0.99754200	1.71540900	-0.08310000
C	1.24420000	0.42013600	0.00046600
C	3.69960700	0.46784900	0.54653100
H	3.92365300	1.23445500	-0.19508400
H	3.61043600	0.92787000	1.53070200
H	4.49870300	-0.27066100	0.56082700
C	-3.34779800	-0.54370900	0.05296300
H	-3.69701700	0.07412500	-0.78093900
H	-4.01343300	-1.39314900	0.18941000
O	-3.37823100	0.20791800	1.25176300
H	-2.92929700	1.04108500	1.07112600

B3LYP-D3BJ

0 1

N	2.55904700	-0.22890800	0.07930300
C	2.27258600	-1.57600800	0.08155800
H	3.03563500	-2.33173600	0.17022100
N	0.92766100	-1.80855000	0.04249800
C	0.36038300	-0.59966700	0.05569400
C	-1.00088000	-0.14596700	-0.14239600
N	-2.02416500	-1.03636300	-0.19013300
H	-1.81634900	-2.00722800	0.00609700
N	-1.26032000	1.16875500	-0.17778400
C	-0.25828600	2.03989400	-0.07623800
H	-0.50151300	3.09290000	-0.05474900
N	1.12153100	1.72422400	-0.08514200
C	1.34361900	0.44343900	0.05020100
C	3.86697300	0.39867100	0.03092600
H	3.98757200	0.94085700	-0.91014200
H	3.97689200	1.09748100	0.86129800
H	4.62955400	-0.37401100	0.10446600
C	-3.39837400	-0.60933600	-0.37412900
H	-3.46071300	-0.06911400	-1.32492600
H	-4.02649400	-1.49541400	-0.40551900
O	-3.85902600	0.21010400	0.68540600
H	-3.33479200	1.02516600	0.63512100

S_{1CTmin} of 9Mehm6A

ωB97X-D3

0 1

N	2.07613700	-0.78127000	0.05479700
C	1.23650700	-1.86009300	0.04810900
H	1.61352900	-2.87120300	0.07947500
N	-0.03726700	-1.52011400	-0.01020000
C	-0.03325800	-0.15885300	-0.04461100
C	-1.10201000	0.82431100	-0.16403700
N	-2.19834800	0.48337900	0.62919900
H	-2.22007900	0.80600000	1.59785800
N	-0.69213200	2.13663600	-0.19507100
C	0.58429100	2.43650700	-0.19021300
H	0.82787500	3.48936300	-0.30454700
N	1.66094900	1.60846500	-0.06099200
C	1.28426700	0.33496200	0.01625100
C	3.52724100	-0.79487500	0.11597600
H	3.93850500	-0.28108800	-0.75301700
H	3.86729000	-0.29923700	1.02544700
H	3.86648800	-1.82919900	0.11928000
C	-3.18898200	-0.52230600	0.26889400

H	-3.49023500	-1.02476100	1.19502000
H	-4.06332200	-0.00075000	-0.14352700
O	-2.74511500	-1.40587400	-0.70249500
H	-1.89284100	-1.78971300	-0.42237900

B3LYP-D3BJ

0 1

N	2.10883700	-0.74563100	0.04149100
C	1.29462300	-1.85498700	0.15437800
H	1.69710400	-2.85360700	0.19888700
N	0.00683400	-1.52555100	0.20257200
C	-0.00992300	-0.15596500	0.12444400
C	-1.07980200	0.78158300	0.00059200
N	-2.27466000	0.38184700	0.65821800
H	-2.31941800	0.45490600	1.67990800
N	-0.76347100	2.11605500	-0.08864100
C	0.50953200	2.44921500	-0.19766800
H	0.70903500	3.50665100	-0.34592000
N	1.62129900	1.65207900	-0.14540000
C	1.29079300	0.35820700	0.02107300
C	3.56210800	-0.73317500	-0.04903000
H	3.87371000	-0.25651600	-0.97898100
H	3.98667300	-0.18674000	0.79380100
H	3.92178100	-1.76018200	-0.03150200
C	-3.24395600	-0.51036200	0.04824600
H	-3.80312000	-0.99201500	0.85653400
H	-3.93766400	0.10723900	-0.54084300
O	-2.64203800	-1.42445600	-0.81488300
H	-1.82391100	-1.78278300	-0.40270900

S_{0min} of 9Mef6A

ωB97X-D3

0 1

C	-3.78705100	0.27231200	-0.02409300
H	-3.92958400	0.87815300	-0.91884700
N	-2.44326200	-0.27991900	-0.00865200
C	-2.08287800	-1.59938200	-0.00542400
H	-2.83366100	-2.37708300	-0.01235400
N	-0.78953600	-1.80226500	0.00646200
C	-0.26170400	-0.53047200	0.01151500
C	1.04793600	-0.03990600	0.02096600
N	2.09343500	-0.94970900	0.02956000
H	1.80236200	-1.91805400	0.05075900
N	1.25498900	1.27039200	0.02448200
C	0.18531200	2.08229800	0.01521000
H	0.40791400	3.14445400	0.01783900
N	-1.09814900	1.74915800	0.00352100
C	-1.27322000	0.42759400	0.00253800
C	3.45149800	-0.74478900	-0.00759100
O	4.02655700	0.31559900	-0.05625900
H	3.98486400	-1.70812300	0.01137100
H	-4.49952000	-0.55021800	-0.02701300
H	-3.94652800	0.88653800	0.86198100

B3LYP-D3BJ

0 1

C	-3.80363900	0.27015500	0.01463200
H	-3.95984400	0.88532500	-0.87137100
N	-2.45400600	-0.28185000	0.00498600
C	-2.09227100	-1.60896600	0.00297700
H	-2.84057000	-2.38764000	0.00693200
N	-0.79062400	-1.80504700	-0.00409100
C	-0.25985000	-0.53043300	-0.00699100

C	1.05207200	-0.03839600	-0.01244900
N	2.10035000	-0.94954700	-0.01726600
H	1.80624700	-1.91866300	-0.02946300
N	1.25917700	1.27844000	-0.01447900
C	0.18793000	2.09220400	-0.00902000
H	0.40785800	3.15432700	-0.01059400
N	-1.10273600	1.75497100	-0.00204600
C	-1.28039300	0.43223400	-0.00154600
C	3.46244000	-0.75061800	0.00469200
O	4.04756200	0.31083500	0.03310600
H	3.98820000	-1.71853500	-0.00618300
H	-4.51416100	-0.55355400	0.01390000
H	-3.95109500	0.87622000	0.90843800

S_{1min} of 9Mef6A

ωB97X-D3

0 1

C	3.69297000	0.56211000	0.00151500
H	3.77988100	1.16571700	0.90518200
N	2.42871800	-0.15248200	-0.00111200
C	2.24157400	-1.50729900	-0.00038000
H	3.07851900	-2.18961200	-0.00054100
N	0.97282400	-1.85405200	-0.00014000
C	0.30418300	-0.66150500	0.00010800
C	-1.08233600	-0.32218000	-0.00002000
N	-2.14779400	-1.15550000	0.00002400
H	-2.00007900	-2.15419600	0.00060000
N	-1.32945800	0.99804800	-0.00044400
C	-0.43042900	1.96050300	-0.00055200
H	-0.79424900	2.98084800	-0.00072300
N	0.88841800	1.73895200	-0.00031200
C	1.18435400	0.41068700	-0.00023500
C	-3.40645900	-0.65448700	0.00028400
O	-3.60134600	0.59637700	0.00066800
H	-4.22600000	-1.37043200	0.00027200
H	4.50365600	-0.16381000	-0.02690700
H	3.75694900	1.20873700	-0.87366700

B3LYP-D3BJ

0 1

C	-3.71018300	0.55752700	0.00046300
H	-3.78628600	1.18743000	-0.88612600
N	-2.43942600	-0.15512500	-0.00020100
C	-2.25104700	-1.52161000	-0.00030600
H	-3.08350600	-2.20682700	-0.00041000
N	-0.96769900	-1.85591600	-0.00003900
C	-0.30035200	-0.66216000	-0.00011300
C	1.08021900	-0.31152400	-0.00002700
N	2.15481100	-1.15405100	0.00017000
H	2.00154500	-2.15355100	-0.00013000
N	1.33572800	1.01477400	-0.00013900
C	0.43597200	1.97514800	-0.00021600
H	0.78869100	2.99829000	-0.00065200
N	-0.89766600	1.74169000	0.00003500
C	-1.19488700	0.41724000	-0.00003700
C	3.41284400	-0.66476000	0.00044700
O	3.62819200	0.58448400	-0.00000800
H	4.22634900	-1.38814400	-0.00037300
H	-4.51792900	-0.17163900	-0.00442700
H	-3.79004700	1.17979400	0.89214500

Reference

1. T. Kobayashi, Y. Harada, T. Suzuki and T. Ichimura, *The Journal of Physical Chemistry A*, 2008,

112, 13308-13315.

2. L. Fu, Z. Wang, Y. Liu, X. Wang, R. Xu, W. Liu, J. Chen and J. Xu, *Journal of Photochemistry and Photobiology A: Chemistry*, 2020, **396**, 112491.
3. Z. Liu, T. Lu and Q. Chen, *Carbon*, 2020, **165**, 461-467.